Title

Rescue of cell death and inflammation of a mouse model of complex 1-mediated vision loss by repurposed drug molecules.

Journal

Human Molecular Genetics, 26(24)

ISSN

0964-6906

Authors

Yu, Alfred K
Datta, Sandipan
McMackin, Marissa Z
et al.

Publication Date

2017-12-15

DOI

10.1093/hmg/ddx373

Peer reviewed

Human Molecular Genetics, 2017, Vol. 26, No. 24 4929–4936

doi: 10.1093/hmg/ddx373
Advance Access Publication Date: 12 October 2017
Original Article

ORIGINAL ARTICLE

Rescue of cell death and inflammation of a mouse model of complex 1-mediated vision loss by repurposed drug molecules

Alfred K. Yu, Sandipan Datta, Marissa Z. McMackin and Gino A. Cortopassi*

Department of Molecular Biosciences, University of California Davis, School of Veterinary Medicine, Davis, CA 95616, USA

*To whom correspondence should be addressed at: Department of Molecular Biosciences, UC Davis, School of Veterinary Medicine, 1089 Veterinary Medicine Drive, Davis, CA 95616, USA. Tel: +15307549665; Fax: +15307549341; Email: gcortopassi@ucdavis.edu

Abstract

Inherited mitochondrial optic neuropathies, such as Leber's hereditary optic neuropathy (LHON) and Autosomal dominant optic atrophy (ADOA) are caused by mutant mitochondrial proteins that lead to defects in mitochondrial complex 1-driven ATP synthesis, and cause specific retinal ganglion cell (RGC) loss. Complex 1 defects also occur in patients with primary open angle glaucoma (POAG), in which there is specific RGC loss. The treatment of mitochondrial optic neuropathy in the US is only supportive. The Ndufs4 knockout (Ndufs4 KO) mouse is a mitochondrial complex 1-deficient model that leads to RGC loss and rapid vision loss and allows for streamlined testing of potential therapeutics. Preceding RGC loss in the Ndufs4 KO is the loss of starburst amacrine cells, which may be an important target in the mechanism of complex 1-deficient vision loss. Papaverine and zolpidem were recently shown to be protective of bioenergetic loss in cell models of optic neuropathy. Treatment of Ndufs4 KO mice with papaverine, zolpidem, and rapamycin-suppressed inflammation, prevented cell death, and protected from vision loss. Thus, in the Ndufs4 KO mouse model of mitochondrial optic neuropathy, papaverine and zolpidem provided significant protection from multiple pathophysiological features, and as approved drugs in wide human use could be considered for the novel indication of human optic neuropathy.

Introduction

Inherited mitochondrial optic neuropathies, such as Leber's hereditary optic neuropathy (LHON) and autosomal dominant optic atrophy (ADOA) are the leading causes of blindness due to mitochondrial protein mutations (1). These inherited diseases lead to neurodegeneration of the retina and optic nerve, and currently there are no treatment options for LHON or ADOA patients in the US, only supportive therapy (2). A defect in mitochondrial complex 1-driven ATP synthesis has been noted in LHON and ADOA cells (3,4). Also, patients with primary open angle glaucoma (POAG) have defects in complex 1-driven ATP synthesis (5), and there is growing evidence that mitochondrial dysfunction may contribute to the pathogenesis of POAG (5–10). In all three diseases, there is preferential death of retinal ganglion cells (RGCs), suggesting a link between mitochondrial complex 1 defects and RGC death. Pathologic symptoms of LHON and ADOA are commonly mistaken for symptoms of glaucoma, which highlights the broader importance of mitochondrial deficiency in optic neuropathy (11).

The Ndufs4 knockout (Ndufs4 KO) mouse is a severe mitochondrial complex 1-deficient model that develops vision loss at P30 (12). The pathological phenotype of the Ndufs4 KO retina includes loss of rod bipolar cells (RBCs) (13), loss of starburst amacrine cells (SBACs) at P24, elevated innate immunity and inflammation and loss of vision at P30 days, and RGC degeneration at P42 days (14). The Ndufs4 KO mouse is an important

Received: June 22, 2017. **Revised:** September 22, 2017. **Accepted:** September 28, 2017

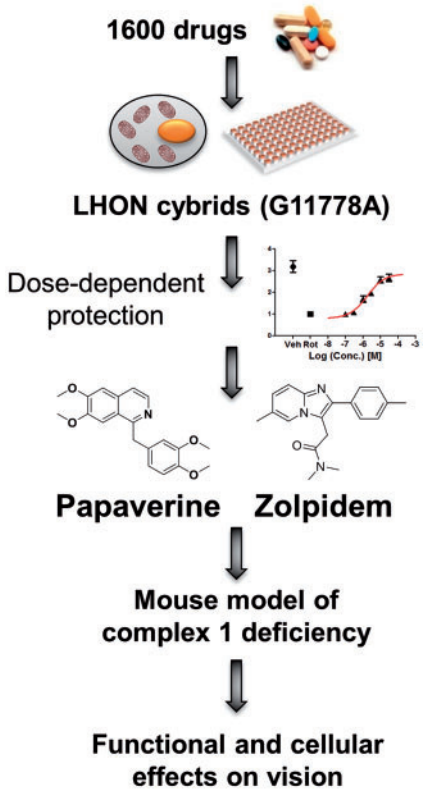

Figure 1. Drug discovery. Papaverine and zolpidem were two drugs discovered from a library of 1600 drugs. They were able to reverse the biochemical defect in mitochondrial deficient cell lines in a dose-dependent manner. These drugs were then used in a complex 1 deficient mouse model.

model in understanding the connection between mitochondrial dysfunction and vision loss. We previously characterized the phenotype of this mouse on the functional, cellular, and molecular level (14). As described in Datta *et al.* (2016), we recently screened the Pharmakon collection of 1600 FDA-approved/clinically-evaluated drugs for their ability to protect from a biochemical defect in mitochondrial complex 1-deficient cells, identifying papaverine and zolpidem as protective (4) (Fig. 1). Here, we tested the effects of papaverine and zolpidem that were protective in the cell model of LHON (4) in a mouse model of complex 1-defciency. In addition, we tested the effects of rapamycin, which extended lifespan in Ndufs4 KO mice (15), and idebenone, which is currently supported as a drug for LHON treatment (16). We observed that papaverine, zolpidem, and rapamycin preserved visual function, protected retinal cells from death, and rescued from an innate immune and inflammatory response that occurs at the time of vision loss. These data suggest that the approved drugs papaverine and zolpidem could be considered as potential therapeutics for human optic neuropathy.

Results

Visual function protection after drug treatment

Papaverine and zolpidem were identified as novel mitochondrial-protective compounds *in vitro* (Fig. 1) (4), and then were dosed at 20 mg/kg i.p. as described in the methods in the Ndufs4 KO mouse model of mitochondrial optic neuropathy that we have previously described (14). Following 2 weeks of drug and vehicle treatment, evaluation of visual function was performed via visual cliff assay (17) (Fig. 2A) in control and Ndufs4 KO mice. Papaverine, zolpidem, and rapamycin significantly preserved the visual function of the Ndufs4 KO mice in the visual cliff assay at P35 (Fig. 2B). Ndufs4 KO mice that received treatment with papaverine, zolpidem, or rapamycin displayed two to three edge detections during a 1-min time frame and showed signs that visual function was intact. In contrast, Ndufs4 KO that received vehicle injections were assessed to be blind and typically displayed zero edge detections. The slow angled-descent forepaw grasping (SLAG) (18) test was also performed after papaverine treatment to confirm visual function protection (Fig. 2C). Treatment with papaverine produced a significant increase in the number of SLAG(+) mice. Additionally, visual function was evaluated by electroretinogram (ERG) and a- and b-wave amplitudes were measured, which confirmed that Ndufs4 KO mice have a reduction in visual function as shown by a significant decrease in a- and b-wave amplitude (Supplementary Material, Fig. S1). However, drug treatments did not produce significant recovery of a- and b-wave amplitudes. Idebenone was not observed to protect in the visual cliff assay.

Starburst amacrine cell protection

We previously demonstrated that starburst amacrine cells (SBACs) are quite sensitive to mitochondrial deficiency (14), possibly because amacrine cells have been shown to have dopaminergic character with greater reliance on mitochondrial function (19). Thus, the ability of drugs to protect SBACs from death was measured. Whole retinas from mice that received either vehicle or drug treatment were collected and processed for immunofluorescent staining with a SBAC-specific ChAT antibody (Fig. 3A–F). Vehicle-treated Ndufs4 KOs had a significant reduction in SBACs (>30% decrease), as expected. Zolpidem and rapamycin significantly protected from SBAC loss (Fig. 3), whereas papaverine produced a trend of increased survival of SBACs, but was not statistically significant. Idebenone did not protect SBACs.

Suppression of innate immunity and inflammation

We previously demonstrated an 'inflammatory wave' that occurred concurrently with vision loss in Ndufs4 KO mice (14), and these transcripts were tested by qRT-PCR. Gene expression of B2m, Tlr2, Cxcl10, Ccl5, Aif1, and Cd68 were evaluated in the Ndufs4 KO retinas. All six of these inflammatory markers are highly elevated in the Ndufs4 KO retina. All four drugs significantly suppressed innate immune markers, B2m and Tlr2 (Fig. 4A and B); and markers of cytokine signaling, Cxcl10 and Ccl5 (Fig. 4C and D). Papaverine, zolpidem, and rapamycin significantly inhibited the expression of microglial activation genes, Aif1 and Cd68 (Fig. 4E and F), idebenone had no significant effect in suppressing microglial activation at the RNA level.

Inhibition of microglial activation

Using whole mount retinas, we measured the expression of Iba1, which is an inflammatory microglial protein encoded by the Aif1 gene, in vehicle and drug-treated mice. We observed increased microglial count and activation in the inner nuclear layer and the inner plexiform layer of the Ndufs4 KO retina, in agreement with our previous observations (14). Additionally, the morphology of the microglia transitioned from a classical resting to an activated state (Fig. 5). Papaverine significantly inhibited microglial activation (reduced the volume of

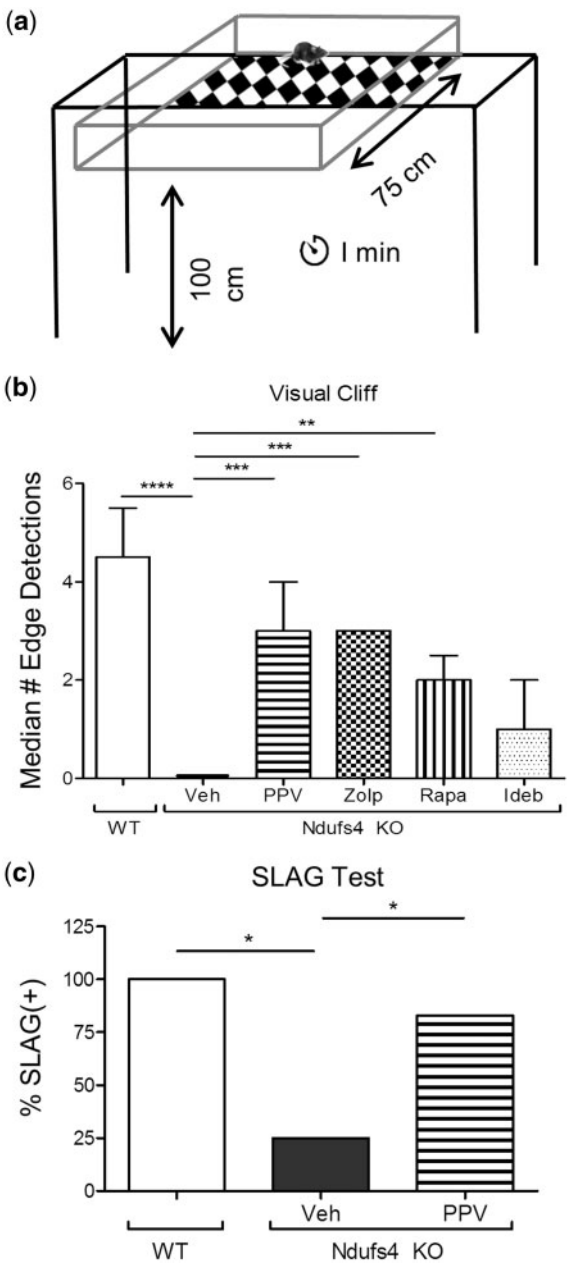

Figure 2. Functional preservation by drug treatment. (**A**) Schematic representation of visual cliff apparatus. (**B**) Graphical representation of the median number of edge detections performed by wild type and vehicle or drug-treated Ndufs4 KO mice. Error bars represent median absolute deviation (zero for vehicle and zolpidem groups). For wild type, Ndufs4 KO Veh, Ndufs4 KO PPV, Ndufs4 KO Zolp, Ndufs4 KO Rapa, and Ndufs4 KO Ideb, $n = 8$, 8, 7, 6, 6, and 5, respectively. Statistical significance determined by two-tailed student's t test. $^{*}P < 0.05$, $^{**}P < 0.01$ $^{***}P < 0.001$, $^{****}P < 0.0001$. (c) Graphical representation of slow angled-descent forepaw grasping (SLAG) in wild type ($n = 4$), Ndufs4 KO veh-treated ($n = 4$), and Ndufs4 KO PPV-treated ($n = 6$) mice. Statistical significance determined by Chi-square analysis. $^{*}P < 0.05$.

Iba1-positive microglia) to wild type control levels; other drugs did not produce statistically significant differences (Fig. 5).

Discussion

Mitochondrial complex 1 defects cause vision loss in LHON, ADOA and POAG. The pathophysiological mechanism has been suggested by others as mitochondrial defects trigger REDD1 transcription, and an inhibition of mTOR, causing RGC death (20,21). The role of mitochondrial deficiency in optic neuropathy is not well understood, and frequently, inherited mitochondrial optic neuropathies are commonly mistaken for symptoms of glaucoma (11), highlighting the heterogeneity among mitochondrial optic neuropathy. To better understand the role of mitochondrial deficiency in optic neuropathy we tested two drugs, papaverine and zolpidem, which were recently shown to protect LHON cells from mitochondrial complex 1-mediated defects in ATP synthesis *in vitro* (4). Additionally, we treated the Ndufs4 KO mice with rapamycin, which has been shown to extend the lifespan of these mice (15); and idebenone which is the only approved treatment for LHON in Europe. Each drug was evaluated on their efficacy in preserving visual function, preventing cell death of SBACs, and suppressing the innate immune and inflammatory response in the retina in the context of complex 1-mediated vision loss.

We took a repurposing approach to drug discovery in which we screened 1600 drugs based on mitoprotective function. Although all these drugs that we tested have different known primary targets, papaverine and zolpidem dosed at higher concentrations target other canonical pathways that stimulate mitochondrial function in a dose-response manner (4). Papaverine has been traditionally used as a vasodilator (22); and zolpidem, a $GABA_A$ agonist, classically used as a sedative (23). This 'target-blind' approach identifies drugs based on their functional effects rather than their suspected targets.

Papaverine, zolpidem, and rapamycin all had effects in the Ndufs4 KO retina that prevented the visual dysfunction observed in vehicle-treated Ndufs4 KOs. Since the usual antecedent of the vision loss, the 'inflammatory wave' was also inhibited, we suggest the mechanism mitochondrial complex 1 defect → cell death → inflammatory wave → vision loss, and that the drugs work to protect mitochondrial bioenergetics at the earliest step (4). In the case of papaverine, there is a very potent suppression of microglial activation, decreasing this parameter down to wild type levels. By contrast, rapamycin's most potent effect was protecting SBACs from death. Zolpidem, although was not the best in inhibiting microglial activation or SBAC apoptosis had an intermediate effect in both of these components, which may underlie its protection from vision loss.

Although there was a noticeable difference in visual function of the Ndufs4 KO mice treated with papaverine, zolpidem, and rapamycin as seen with visual cliff and SLAG assay there were no major improvements in a- and b-wave amplitudes in ERG that correspond to outputs of photoreceptors and bipolar cells, respectively (24). Our previous study showed that SBACs were the earliest cells to degenerate (14), thus the improved vision could be the result of protection of the direction-selective SBACs and decreased inflammation. The full-field ERG is not tuned to assess the contributions of the inner retina (RGCs and amacrine cells), however measurements of oscillatory potentials provide information about neural interactions of the proximal retina among the bipolar cells, amacrine cells, and ganglion cells (25). Similar to the a- and b-wave, the oscillatory potentials were not statistically different in vehicle- versus drug-treated Ndufs4 KO retinas (Supplementary Material).

Aside from RGCs in the ganglion cell layer (GCL), the only other neurons are displaced amacrine cells, which account for ~50% of the cells in rodent GCL. Specifically, SBACs account for ~20% of all the displaced amacrines (26). An analysis of the GCL in primates reported that displaced amacrine cells make up

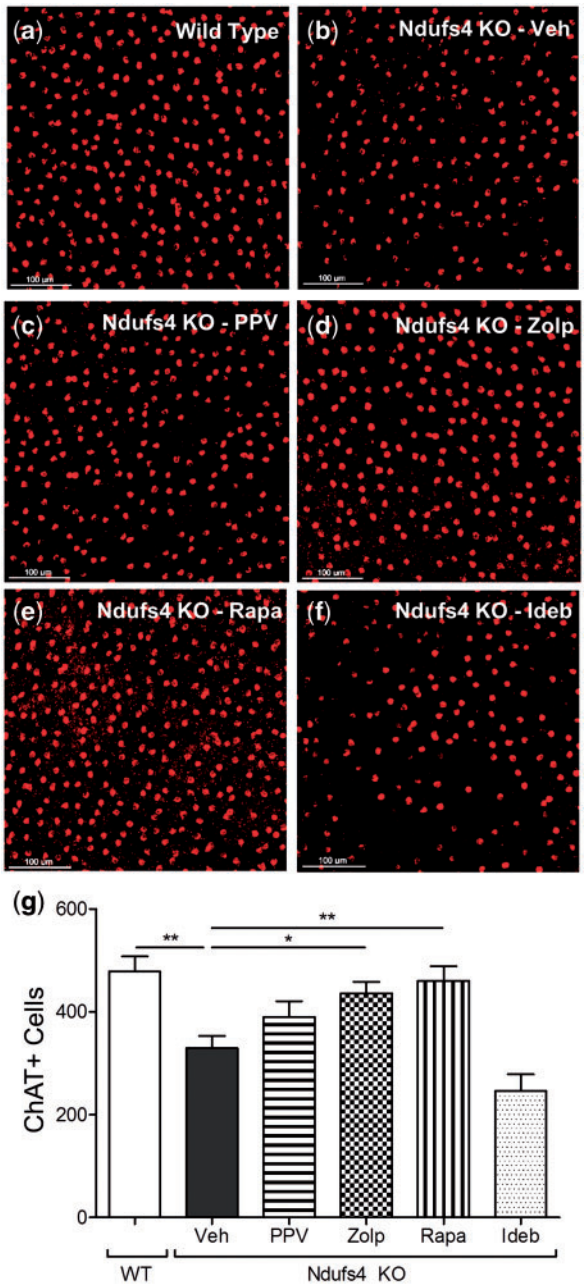

Figure 3. Prevention of cell apoptosis. Representative 20x images of ChAT-positive (red) cell from retinas of: (**A**) wild type vehicle treated, (**B**) Ndufs4 KO vehicle treated, (**C**) Ndufs4 KO papaverine treated, (**D**) Ndufs4 KO zolpidem treated, (**E**) Ndufs4 KO rapamycin treated, and (**F**) Ndufs4 KO idebenone treated. (**G**) graphical representation of mean number of ChAT-positive cells. Error bars represent standard error of the mean. For wild type, Ndufs4 KO Veh, Ndufs4 KO PPV, Ndufs4 KO Zolp, Ndufs4 KO Rapa, and Ndufs4 KO Ideb, $n = 8, 8, 7, 6, 6$, and 5, respectively. Statistical significance determined by two-tailed student's t test. $^{*}P < 0.05$, $^{**}P < 0.01$.

~6% of total neurons in the central region of the retina and ~70% in the periphery (27). Their close proximity to and direct connectivity to RGCs play a key role in RGC functionality. In LHON it is observed that the GCL and inner plexiform layer are significantly decreased (28–30), however, RGC loss may be mediated by other retinal cell types. Therefore, it is important to look more closely at the importance of amacrine cells in visual function, and how drugs affect their survival in the Ndufs4 KO.

At the cellular level, we examined the effect of drug on the SBACs because there is a significant loss of this cell population in the retina even before vision loss and RGC death is observed (14). SBACs are interneurons in the retina that are important in signal transduction (31). SBACs receive input from bipolar cell terminals and synapse onto ganglion cells or other amacrine cells. During development SBACs are important in the formation of visual circuits. After development SBACs have a primary role in generating directional signals relayed to direction-selective ganglion cells. SBACs uniquely release excitatory (acetylcholine) and inhibitory (GABA) neurotransmitters (31). Additionally, it has been found that mitochondrial complex 1 inhibition by rotenone causes a preferential loss of dopaminergic amacrine cells (19,32). Although the hallmark characteristic of LHON, ADOA, and POAG is ganglion cell loss, the pathophysiological mechanism in the Ndufs4 KO suggest that the key cell types affected prior to vision loss are SBACs and bipolar cells (13), and that these cell types should be potential targets of interest in developing therapeutics.

In humans with ADOA, inherited OPA1 deficiency causes a decrease in mitochondrial function and vision loss. We observed a consistent Opa1 deficiency in Ndufs4 KO mice (14). It has been reported that the OPA1 gene (the defect of which causes ADOA) is important in RGC and amacrine cell function. Additionally, there has been a link between the mitochondrial protein, OPA1, and SBACs in intrinsic signal processing of the inner retina (33). We hypothesize that the inflammation may be a response to cell death of SBACs as a result of vulnerability to the mitochondrial bioenergetic defect. The loss of SBACs then initiates the decline in signal transduction and visual function. This is further supported by an increase in microglia in the inner nuclear layer and the ganglion cell layer, where the SBACs reside, to phagocytize apoptotic cells (14). Retinal ganglion cells were not examined in these experiments since there were no changes in cell count at the time of vision loss (14). Also, the death of SBACs precedes functional loss and we wanted to target cells that are affected prior to vision loss to effectively prevent it from occurring.

In the Ndufs4 KO, it is clear that inflammation is playing a key role in the neurodegeneration of the retina and that the peak of inflammation is occurring right before or at the time of vision loss in these mice, which further supports the need of drugs that are able to inhibit the inflammatory response. In LHON and ADOA patients, there has been a report of the presence of macular microcysts, which have been observed in inflammatory optic neuritis and suggest an inflammatory nature to mitochondrial optic neuropathies (34). Similarly, neuroinflammation has been reported to be a major contributing factor to the mechanism of glaucoma (35,36), further suggesting similar pathological mechanisms between LHON, ADOA, and POAG. We do not believe that papaverine and zolpidem are acting primarily as anti-inflammatory molecules, but are working to protect mitochondria function in the context of complex 1 deficiency and thereby suppressing the inflammatory response.

Currently, the approved treatment for LHON in Europe is idebenone, so we analyzed the effect of systemic idebenone in the Ndufs4 KO retina. Idebenone inhibited cytokine signaling (Cxcl10and Ccl5) significantly, providing some suggestion of protection; however, did not decrease microglial activation. In addition, idebenone had no effect in preserving SBACs. Idebenone was dosed in Ndufs4 KO mice at more than 10-fold higher concentration (200 mg/kg) than that given in human clinical trials (11.25 mg/kg; given an 80 kg adult) (16). Idebenone did have a strong effect in inhibiting the cytokine signaling as seen

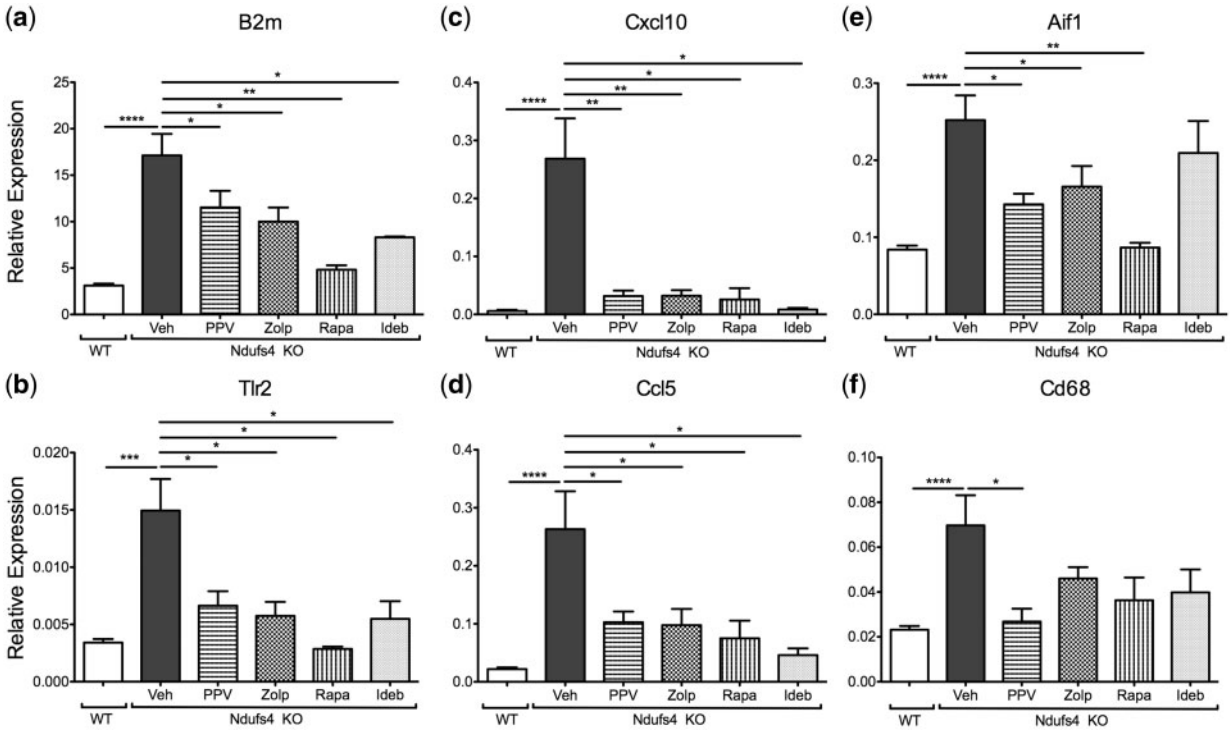

Figure 4. Inhibition of innate immunity and inflammation. Graphical representation of RNA expression of (**A**) B2m, (**B**) Tlr2, (**C**) Cxcl10, (**D**) Ccl5, (**E**) Aif1, and (**F**) Cd68. Bars represent mean delta Ct values normalized to housekeeping genes, Actb and Mapk1. Error bars represent standard error of the mean. For wild type, Ndufs4 KO Veh, Ndufs4 KO PPV, Ndufs4 KO Zolp, Ndufs4 KO Rapa, and Ndufs4 KO Ideb, $n = 8$, 8, 7, 6, 6, and 5, respectively. Statistical significance determined by two-tailed student's t test. *$P < 0.05$, **$P < 0.01$, ****$P < 0.0001$.

with Cxcl10 and Ccl5, demonstrating that the dose is having an effect in the mouse retina, however that did not translate into functional preservation or cellular protection. Similarly, in a mouse model of ADOA, idebenone treatment was ineffective in protecting RGCs from dendropathy (37).

Papaverine is the most potent molecule shown to protect the LHON-specific ATP synthesis defect *in vitro* (4), it also protects visual function in the Ndufs4 KO mice as confirmed by visual function assays, and is the most potent inhibitor of retinal inflammation as determined by suppression of microglial activation. Furthermore, moxaverine, a papaverine analog has been tested in human and rabbit subjects and has shown to increase ocular blood flow, indicating that the drug reaches the posterior region of the eye when given systemically and topically via eye drops (38,39). These preclinical data suggest that papaverine and its analogs could be considered for the treatment of mitochondrial vision loss. Papaverine is not currently approved in the USA, but is approved in Europe as an injectable.

Zolpidem also known as Ambien, is in general use in the USA as an orally-dosed sleep aid. Zolpidem significantly protected SBACs from death and from complex 1-dependent increase in inflammatory transcripts. Because of its approved status in the USA and elsewhere, and its protective nature in LHON cells and the mouse model of optic neuropathy, zolpidem could be considered for complex 1-dependent optic neuropathy. Additionally, it is possible that zolpidem could be administered intraocularly rather than systemically, thus focusing the effect on the retina with minimal sedative effects.

Papaverine and zolpidem were previously shown to increase ATP synthesis in complex 1-deficient cells *in vitro* (4). The mechanism by which both are acting is still largely unknown, but we believe that papaverine is acting through a compensatory mechanism to increase complex 2 activity by direct targeting a cytosolic or plasma membrane target; and zolpidem is acting to restore complex 1 activity through a cytosolic or plasma membrane target (Supplementary Material) (4). In Yu *et al.* (2015) we described two possible causes of complex 1-mediated cell death. The first was necrosis, i.e. complex 1 defect → amacrine cell death → inflammation → vision loss. The second was complex 1 misfolding → mitochondrial innate immune response → inflammation → vision loss (14). We test the second idea of increased 'mitochondrial innate immune response' by quantifying these recently described transcripts (cGas, STING, IRG3, TBK1 - data not shown) (40). However, after finding no statistically significant increase in these transcripts in the Ndufs4 KO, we concluded that this second pathway is unlikely to be correct and now favor the first hypothesis.

Here we showed by dosing these approved drugs *in vivo* that vision loss is suppressed, SBACs were protected from death, and the inflammatory and innate immune and microglial reactivity caused by the mitochondrial defects was reduced, in some cases to the wild type level. Papaverine and zolpidem are potential novel therapeutics for complex 1-deficiency driven optic neuropathy as seen in LHON, ADOA, and POAG, because of their mitoprotective function *in vitro* and protection from mitochondrial deficiency *in vivo*. They are approved in either US or Europe or both, and zolpidem is conveniently available as an orally-dosed agent, and these two drugs could be considered for human clinical trials for effectiveness in mitochondrial optic neuropathies. This is just a starting point in which future directions will be aimed at developing more potent analogs of these drugs with reduced side effects and to also consider combinations of these drugs as it is expected that there would be an additive effect of treatment with papaverine and zolpidem

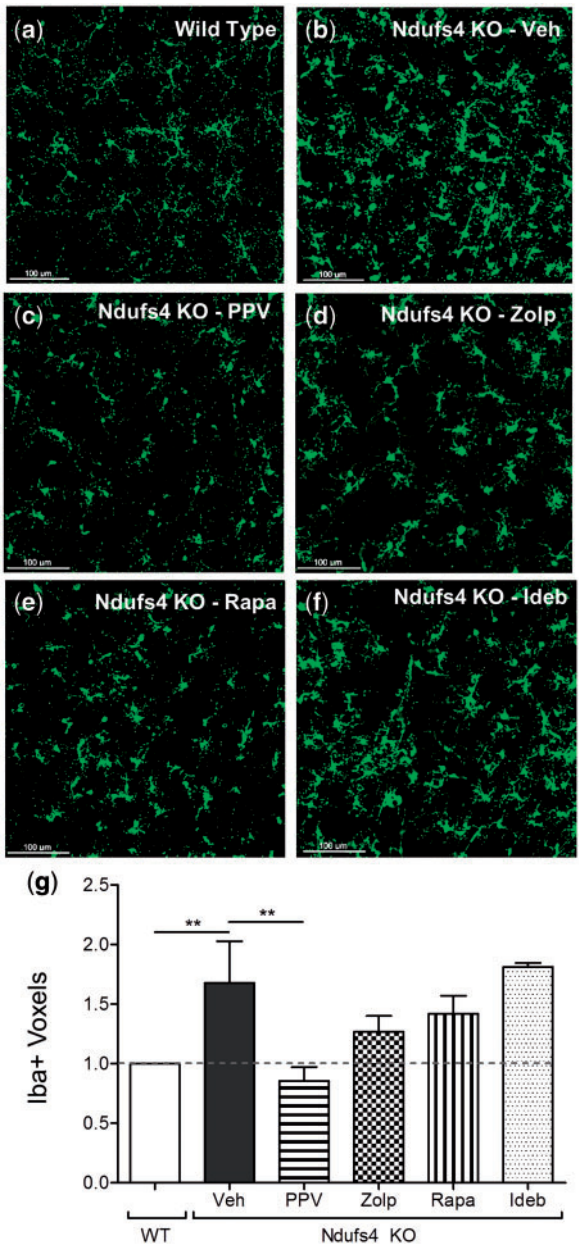

Figure 5. Microglia inhibition by papaverine. 20x confocal z-stack of Iba1-positive (green) microglia in the inner nuclear layer and inner plexiform layer of (**A**) Ndufs4 wild type, (**B**) Ndufs4 KO Veh, (**C**) Ndufs4 KO PPV, (**D**) Ndufs4 KO Zolp, (**E**) Ndufs4 KO Rapa, and (**F**) Ndufs4 KO Ideb. (**G**) Graphical representation of mean Iba1-positive microglia volume measured in voxels. Error bars represent standard error of the mean. For wild type, Ndufs4 KO Veh, Ndufs4 KO PPV, Ndufs4 KO Zolp, Ndufs4 KO Rapa, and Ndufs4 KO Ideb, $n = 8$, 8, 7, 6, 6, and 5, respectively. Statistical significance determined by two-tailed student's *t* test. $^{**}P < 0.01$.

since their beneficial effects are acting through different mechanisms.

Materials and Methods

Animal

The Ndufs4 KO mice were generously gifted from Zhengui Xia and Richard Palmiter from the University of Washington. All experiments were performed in accordance with the National Institutes of Health and institutional guidelines regarding animal use and were approved by the Animal Care and Use Committee of the University of California, Davis (IACUC). Animals were housed in an approved animal facility and food and water was provided *ad libitum*. Mice were weaned at postnatal 21 days (P21) at which time they would be placed in drug groups to receive systemic intraperitoneal injects of either vehicle or one of four drugs (papaverine, zolpidem, rapamycin, or idebenone). The number of wild type mice used was 8 and the numbers of Ndufs4 KO mice were 8 vehicle treated, 7 papaverine treated, 6 zolpidem treated, 6 rapamycin treated, and 5 idebenone treated.

Drug formulation

Papaverine, zolpidem, and rapamycin was dissolved in DMSO and diluted with PBS (0.5% DMSO), 5% PEG-400, and 5% Tween-20 to a reach a dose of 20 mg/kg for papaverine and zolpidem, and 8 mg/kg for rapamycin. The solution was then sterile filtered, aliquoted, and stored at -80 °C for long-term storage. Idebenone powder was mixed with a gelatin solution to a dose of 200 mg/kg and formed into a jelly that the mice consumed orally. Jelly portions were consumed within 5 min of placing the jelly in the cage. Doses were administered everyday starting at P21 and ending at P35.

Visual cliff

A clear 75 × 75 cm acrylic box was constructed with a checkered board pattern on 1/3 of the box and the remainder of the box was clear and hung over a table. The same checkerboard pattern was placed on the floor 100 cm below the box to create a sense of depth, this created an illusion of a 'cliff.' To start the test a mouse was placed on the back end of the box furthest away from the 'cliff' (17). The mouse was allowed to move freely and was recorded on video for analysis. A 1-min time period was initiated once the mouse reached the 'cliff'. Analysis of the videos involved counting the number edge detections (arrive at edge, hesitate, and move away from edge) in that 1-min period. Blind analysis of randomized videos was performed by two investigators (Alfred Yu and Marissa McMackin) to remove bias. Significance was determined by two-tailed Student's *t*-Test, $^{*}P < 0.05$, $^{**}P < 0.01$, $^{***}P < 0.001$, and $^{****}P < 0.0001$.

Slow angled-descent forepaw grasping (SLAG)

After visual cliff testing, visual function was confirmed by slow angled-descent forepaw grasping (SLAG) test (18). A clean stainless-steel cage lid was placed on a counter top with one edge placed at an upward angle. Each mouse was suspended by their tail above the cage lid and was slowly lowered diagonally passing over the edge of the wire cage. The cage lid remained in the mouse's visual field throughout the descent. Each mouse was kept at a distance away from the cage lid that prohibited their whiskers from making contact with the cage lid. SLAG(+) mice displayed a directed and sustained reaching of the forepaws toward the edge of the cage lid, whereas, SLAG(-) mice did not display this behavior. Statistical significance was determined by Chi-square analysis, $^{*}P < 0.05$.

Electroretinogram

Mice were dark adapted overnight prior to ERG testing. Mice were then anesthetized with ketamine and xylazine and their eyes were dilated with 1% tropicamide and 2.5% phenylephrine.

Proparacaine (0.5%) was applied to the eyes as a topical anesthetic. Thirty-gauge needle electrodes were inserted under the skin at the base of the tale as a ground and at the top of the skull as a reference. Eyes were lubricated with 1% methylcellulose before contact electrodes were placed on the eye. ERGs were generated with the following program: scotopic white flash 9.95×10^{-6}, 9.95×10^{-5}, 9.95×10^{-4}, 9.95×10^{-3}, 9.95×10^{-2}, 0.995, 2.5, and 9.95 cd•s/m^2, followed by a 10-min period of light adaptation (80 cd/mm background white light) and then photopic white flashes, 9.95×10^{-2}, 0.396, 0.995, 2.5, 9.95 cd•s/m^2. The last step was a photopic white flicker 2.5 cd•s/m^2 at flicker rate of 30.3 Hz. Each waveform was averaged from 5 different flashes with 5 s between each flash. Post hoc analysis was performed by measuring the a-wave (baseline to a-wave trough) and b-wave (a-wave trough to b-wave peak) amplitudes. Significance was determined by two-tailed Student's *t*-test, $^{*}P<0.05$, $^{**}P<0.01$, $^{***}P<0.001$, and $^{****}P<0.0001$.

qRT-PCR

Retinas were surgically extracted from each mouse and placed in RNALater. RNA was isolated from the retinas by column purification (Qiagen). cDNA was then synthesized (Bio-RAD) and used in qRT-PCR. Primer template (Supplementary Material), SensiFast mastermix (Bioline), and cDNA were combined for a final volume of 10 microliters. Fluorescence of the qRT-PCR product was detected by SYBR green using the LightCyler 480 (Roche). Cycle threshold (Ct) value was then converted to delta delta Ct of the target of interest over housekeeping genes (Actb and Mapk1). Significance was determined by two-tailed Student's *t*-test, $^{*}P<0.05$, $^{**}P<0.01$, $^{***}P<0.001$, and $^{****}P<0.0001$.

Immunofluorescence

Whole eyes from mice were surgically extracted and punctured with a 30 g needle at the nasal limbus and then placed in 4% paraformaldehyde for 30 min. Retinas were then removed from the eye by dissecting off the cornea and removing the lens. Four slits were cut into the retina to create a petal shape and orientation was maintained by notching the nasal leaflet. The retinal cup was then placed in fresh 4% paraformaldehyde for 40 min. Retinas were then washed with PBS. Blocking was applied to the retina overnight, followed by primary antibody (ChAT and Iba1) for 2 days. Retinas were then washed well with PBS-Tween and secondary antibody was applied and incubated overnight. Retinas were washed in PBS-Tween for two days and DAPI counterstain was applied for 10 min. Retinas were then flattened onto a slide with fluorescent mounting media and sealed with a coverslip. Retinas were then imaged using the Leica TCS SP8 confocal microscope. Z-stacks were set beginning at the innermost portion of the inner nuclear layer and ending at the end of the ganglion cell layer. 3 D images were then analyzed with Imaris software. In the software, the spots tool was used to count ChAT-positive SBACs and the surface tool was used to create surfaces of the Iba1-positive microglia and the surface volume was measured in voxels. Significance was determined by two-tailed Student's *t*-test, $^{*}P<0.05$, $^{**}P<0.01$, $^{***}P<0.001$, and $^{****}P<0.0001$.

Supplementary Material

Supplementary Material is available at *HMG* online.

Conflict of Interest statement. None declared.

Funding

National Eye Institute (R01 EY0 12245).

References

1. Yu-Wai-Man, P., Votruba, M., Burte, F., La Morgia, C., Barboni, P. and Carelli, V. (2016) A neurodegenerative perspective on mitochondrial optic neuropathies. *Acta Neuropathol.*, **132**, 789–806.
2. Lopez Sanchez, M.I.G., Crowston, J.G., Mackey, D.A. and Trounce, I.A. (2016) Emerging Mitochondrial Therapeutic Targets in Optic Neuropathies. *Pharmacol. Ther.*, **165**, 132–152.
3. Zanna, C., Ghelli, A., Porcelli, A.M., Karbowski, M., Youle, R.J., Schimpf, S., Wissinger, B., Pinti, M., Cossarizza, A., Vidoni, S. *et al.* (2008) OPA1 mutations associated with dominant optic atrophy impair oxidative phosphorylation and mitochondrial fusion. *Brain*, **131**, 352–367.
4. Datta, S., Tomilov, A. and Cortopassi, G. (2016) Identification of small molecules that improve ATP synthesis defects conferred by Leber's hereditary optic neuropathy mutations. *Mitochondrion*, **30**, 177–186.
5. Lee, S., Sheck, L., Crowston, J.G., Van Bergen, N.J., O'Neill, E.C., O'Hare, F., Kong, Y.X.G., Chrysostomou, V., Vincent, A.L. and Trounce, I.A. (2012) Impaired complex-I-linked respiration and ATP synthesis in primary open-angle glaucoma patient lymphoblasts. *Invest Ophthalmol. Vis. Sci.*, **53**, 2431–2437.
6. Izzotti, A., Longobardi, M., Cartiglia, C., Saccà, S.C. and Lewin, A. (2011) Mitochondrial damage in the trabecular meshwork occurs only in primary open-angle glaucoma and in pseudoexfoliative glaucoma. *PLoS One*, **6**, e14567.
7. Collins, D.W., Gudiseva, H.V., Trachtman, B., Bowman, A.S., Sagaser, A., Sankar, P., Miller-Ellis, E., Lehman, A., Addis, V. and O'Brien, J.M. (2016) Association of primary open-angle glaucoma with mitochondrial variants and haplogroups common in African Americans. *Mol. Vis.*, **22**, 454–471.
8. Van Bergen, N.J., Crowston, J.G., Craig, J.E., Burdon, K.P., Kearns, L.S., Sharma, S., Hewitt, A.W., Mackey, D.A., Trounce, I.A. and Vavvas, D. (2015) Measurement of Systemic Mitochondrial Function in Advanced Primary Open-Angle Glaucoma and Leber Hereditary Optic Neuropathy. *PLoS One*, **10**, e0140919.
9. Khawaja, A.P., Cooke Bailey, J.N., Kang, J.H., Allingham, R.R., Hauser, M.A., Brilliant, M., Budenz, D.L., Christen, W.G., Fingert, J. and Gaasterland, D. (2016) Assessing the association of mitochondrial genetic variation with primary open-angle glaucoma using gene-set analyses. *Invest. Ophthalmol. Vis. Sci.*, **57**, 5046–5052.
10. Bosley, T.M., Hellani, A., Spaeth, G.L., Myers, J., Katz, L.J., Moster, M.R., Milcarek, B. and Abu-Amero, K.K. (2011) Down-regulation of OPA1 in patients with primary open angle glaucoma. *Mol. Vis.*, **17**, 1074–1079.
11. Buono, L.M., Foroozan, R., Sergott, R.C. and Savino, P.J. (2002) Is normal tension glaucoma actually an unrecognized hereditary optic neuropathy? New evidence from genetic analysis. *Curr. Opin. Ophthalmol.*, **13**, 362–370.
12. Kruse, S.E., Watt, W.C., Marcinek, D.J., Kapur, R.P., Schenkman, K.A. and Palmiter, R.D. (2008) Mice with mitochondrial complex I deficiency develop a fatal encephalomyopathy. *Cell Metab.*, **7**, 312–320.
13. Song, L., Yu, A., Murray, K. and Cortopassi, G. (2017) Bipolar cell reduction precedes retinal ganglion neuron loss in a complex 1 knockout mouse model. *Brain Res.*, **1657**, 232–244.

14. Yu, A.K., Song, L., Murray, K.D., van der List, D., Sun, C., Shen, Y., Xia, Z. and Cortopassi, G.A. (2015) Mitochondrial complex I deficiency leads to inflammation and retinal ganglion cell death in the Ndufs4 mouse. *Hum. Mol. Genet.*, **24**, 2848–2860.
15. Johnson, S.C., Yanos, M.E., Kayser, E.-B., Quintana, A., Sangesland, M., Castanza, A., Uhde, L., Hui, J., Wall, V.Z., Gagnidze, A. *et al.* (2013) mTOR inhibition alleviates mitochondrial disease in a mouse model of Leigh syndrome. *Science*, **342**, 1524–1528.
16. Klopstock, T., Yu-Wai-Man, P., Dimitriadis, K., Rouleau, J., Heck, S., Bailie, M., Atawan, A., Chattopadhyay, S., Schubert, M., Garip, A. *et al.* (2011) A randomized placebo-controlled trial of idebenone in Leber's hereditary optic neuropathy. *Brain*, **134**, 2677–2686.
17. Pinto, L.H. and Enroth-Cugell, C. (2000) Tests of the mouse visual system. *Mammalian Genome*, **11**, 531–536.
18. Gil-Pages, M., Stiles, R.J., Parks, C.A., Neier, S.C., Radulovic, M., Oliveros, A., Ferrer, A., Reed, B.K., Wilton, K.M. and Schrum, A.G. (2013) Slow angled-descent forepaw grasping (SLAG): an innate behavioral task for identification of individual experimental mice possessing functional vision. *Behav. Brain Funct.*, **9**, 35.
19. Esteve-Rudd, J., Fernandez-Sanchez, L., Lax, P., De Juan, E., Martín-Nieto, J. and Cuenca, N. (2011) Rotenone induces degeneration of photoreceptors and impairs the dopaminergic system in the rat retina. *Neurobiol. Dis.*, **44**, 102–115.
20. Di Polo, A. (2015) Dendrite pathology and neurodegeneration: focus on mTOR. *Neural Regen.Res.*, **10**, 559–561.
21. Morgan-Warren, P.J., Berry, M., Ahmed, Z., Scott, R.A.H. and Logan, A. (2013) Exploiting mTOR signaling: a novel translatable treatment strategy for traumatic optic neuropathy? *Invest. Ophthalmol. Vis. Sci.*, **54**, 6903–6916.
22. Abusnina, A. and Lugnier, C. (2017) Therapeutic potentials of natural compounds acting on cyclic nucleotide phosphodiesterase families. *Cell. Signal.*, **39**, 55–65.
23. Fitzgerald, A.C., Wright, B.T. and Heldt, S.A. (2014) The behavioral pharmacology of zolpidem: evidence for the functional significance of α1-containing GABAA receptors. *Psychopharmacology*, **231**, 1865–1896.
24. Weymouth, A.E. and Vingrys, A.J. (2008) Rodent electroretinography: methods for extraction and interpretation of rod and cone responses. *Prog. Retin. Eye Res.*, **27**, 1–44.
25. Hancock, H.A. and Kraft, T.W. (2004) Oscillatory potential analysis and ERGs of normal and diabetic rats. *Invest. Ophthalmol. Vis. Sci.*, **45**, 1002.
26. Jeon, C.J., Strettoi, E. and Masland, R.H. (1998) The major cell populations of the mouse retina. *J. Neurosci.*, **18**, 8936–8946.
27. Muniz, J.A.P.C., de Athaide, L.M., Gomes, B.D., Finlay, B.L., Silveira, L.C. and de, L. (2014) Ganglion cell and displaced amacrine cell density distribution in the retina of the howler monkey (Alouatta caraya). *PLoS One*, **9**, e115291.
28. Balducci, N., Savini, G., Cascavilla, M.L., La Morgia, C., Triolo, G., Giglio, R., Carbonelli, M., Parisi, V., Sadun, A.A., Bandello, F. *et al.* (2016) Macular nerve fibre and ganglion cell layer changes in acute Leber's hereditary optic neuropathy. *Br. J. Ophthalmol.*, **100**, 1232–1237.
29. Moster, S.J., Moster, M.L., Scannell Bryan, M. and Sergott, R.C. (2016) Retinal ganglion cell and inner plexiform layer loss correlate with visual acuity loss in LHON: a longitudinal, segmentation OCT analysis. *Invest. Ophthalmol. Vis. Sci.*, **57**, 3872–3883.
30. Lam, B.L., Burke, S.P., Wang, M.X., Nadayil, G.A., Rosa, P.R., Gregori, G., Feuer, W.J., Cuprill-Nilson, S., Vandenbroucke, R., Zhang, X. *et al.* (2016) Macular retinal sublayer thicknesses in G11778A Leber hereditary optic neuropathy. *Ophthalmic Surg. Lasers Imaging Retina*, **47**, 802–810.
31. TAYLOR, W.R. and SMITH, R.G. (2012) The role of starburst amacrine cells in visual signal processing. *Vis. Neurosci.*, **29**, 73–81.
32. Biehlmaier, O., Alam, M. and Schmidt, W.J. (2007) A rat model of Parkinsonism shows depletion of dopamine in the retina. *Neurochem. Int.*, **50**, 189–195.
33. Pesch, U.E.A., Fries, J.E., Bette, S., Kalbacher, H., Wissinger, B., Alexander, C. and Kohler, K. (2004) OPA1, the disease gene for autosomal dominant optic atrophy, is specifically expressed in ganglion cells and intrinsic neurons of the retina. *Invest. Ophthalmol. Vis. Sci.*, **45**, 4217–4225.
34. Carbonelli, M., La Morgia, C., Savini, G., Cascavilla, M.L., Borrelli, E., Chicani, F., do V F Ramos, C., Salomao, S.R., Parisi, V., Sebag, J. *et al.* (2015) Macular microcysts in mitochondrial optic neuropathies: prevalence and retinal layer thickness measurements. *PLoS One*, **10**, e0127906.
35. Mac Nair, C.E. and Nickells, R.W. (2015) Neuroinflammation in glaucoma and optic nerve damage. *Prog. Mol. Biol. Transl. Sci.*, **134**, 343–363.
36. Vohra, R., Tsai, J.C. and Kolko, M. (2013) The role of inflammation in the pathogenesis of glaucoma. *Surv. Ophthalmol.*, **58**, 311–320.
37. Smith, T.G., Seto, S., Ganne, P. and Votruba, M. (2016) A randomized, placebo-controlled trial of the benzoquinone idebenone in a mouse model of OPA1-related dominant optic atrophy reveals a limited therapeutic effect on retinal ganglion cell dendropathy and visual function. *Neuroscience*, **319**, 92–106.
38. Pemp, B., Garhofer, G., Lasta, M., Schmidl, D., Wolzt, M. and Schmetterer, L. (2012) The effects of moxaverine on ocular blood flow in patients with age-related macular degeneration or primary open angle glaucoma and in healthy control subjects. *Acta Ophthalmol.*, **90**, 139–145.
39. Becker, U., Ehrhardt, C., Schaefer, U.F., Gukasyan, H.J., Kim, K.-J., Lee, V.H.L. and Lehr, C.-M. (2005) Tissue distribution of moxaverine-hydrochloride in the rabbit eye and plasma. *J. Ocul. Pharmacol. Ther.*, **21**, 210–216.
40. West, A.P., Khoury-Hanold, W., Staron, M., Tal, M.C., Pineda, C.M., Lang, S.M., Bestwick, M., Duguay, B.A., Raimundo, N., MacDuff, D.A. *et al.* (2015) Mitochondrial DNA stress primes the antiviral innate immune response. *Nature*, **520**, 553–557.